Antibacterial Activity of Iron Oxide Nanoparticles Synthesized by Pulsed Laser Ablation AgainstPathogenic Bacteria Isolated from Diabetic Foot Ulcer

Shahad J. Mohammed[1], HaidarKadum Yakob[1], Asmiet Ramizy[2]
[1]Department of Biology, College of Education for Pure Sciences, University Of Anbar, Iraq.
[2]Department of Physics, College of Science, University Of Anbar, Iraq
Corresponding author: asmat_hadithi@uoanbar.edu.iq

Abstract

Diabetic foot ulcer causing bacteria are one of the most important pathogens and considered a serious threat to public health in recent years. The purpose of the study is to investigate the antibacterial activity of iron oxide nanoparticles synthesized by pulsed laser ablation (Fe_2O_3NPs) against some pathogenic bacteria isolated from diabetic patients with recurrent diabetic foot in Baghdad Teaching Hospital, Iraq.

Fifty clinical specimens were collected from each diabetic foot ulcer using sterile swabs and cultured on different culture media. The isolated bacteria were identified based on their cultural and microscopic characteristics, and biochemical tests. Moreover, diagnosis was confirmed using Vitek2 system.Fe_2O_3NP was prepared using pulsed laser ablation. A Nd:YAG (New Wave Research, 1845L) aluminum yttrium garnet laser (New Wave Research, 1845L) focuses on aniron plate surface with a wavelength of 532 nm, energy of 100 mJ, and a laser stroke of 500, 1000, and 1500. The modulated frequency is 6 Hz. As for the distance between the laser device and the iron target surface, 12 cm. During the imaging process, the glass beaker containing the iron plate is periodically transferred to obtain homogeneous colloidal Fe_2O_3NPs. Characterization of the biocompatible Fe_2O_3NPs was performed using scanning field emission electron microscopy (FESEM), UV visible and X-ray diffraction spectroscopy. (XRD). The efficacy of the prepared Fe_2O_3NPs against isolated bacteria was examined using the disc diffusion method.Fifty-two bacterial isolates were obtained. All the prepared iron oxide nanoparticles were found to have antibacterial activities. Fe_2O_3NPs ata laser stroke of 500 were found to have higher antibacterialactivitiesin comparison to the other prepared nanoparticles.Thediametersof the inhibition zone were (25.3±0.6,24.3±0.6,23.8±0.3,18.7±0.6,18.5±0.5,17.5±0.9,16.0±0.9,15.8±0.8,15.7±0.6,15.2±0.3,15.2±0.3,10.3±0.6) mm for nanoparticles (500 laser stroke) against*Proteus vulgaris*, *Proteus penneri, Sphingomonaspaucimobilis, Kocuriakristinae, Staphylococcus aureus, Proteus mirabilis, Klebsiella pneumoniae,Staphylococcus hominis, Escherichia coli,Pseudomonas aeruginosa, Enterococcus faecalis, Aeromonashydrophila,* respectively. In conclusion, the results obtained clearly supported that Fe_2O_3NPs might have potential as antibacterial.

Keywords:Iron oxide nanoparticles, pulsed laser, antibacterial, diabetic foot ulcer.
DOI Number: 10.14704/nq.2022.20.11.NQ66092 **NeuroQuantology 2022; 20(11): 958-970**

Introduction

The synthesis of nanoparticles has been rapidly developed over the past few decades. Iron is one of the metals commonly synthesized into nanoparticles[1].Iron oxide nanoparticles (Fe_2O_3NPs) have been widely employed for various applications, especially in the drug

eISSN 1303-5150

and medications sector such as contrast agent, soft tissue repair, drug delivery, detoxification, immunoassay examination, and cell separation. All of those applications require extremely small size iron particles ranging from 1-100 nm[2]including superparamagnetism, biodegradability, biocompatibility[3]high surfacearea, and stability[4]. Accordingly, increased demand for Fe_2O_3NPssuggests changes in the traditional chemical, physical, and biological synthesis, aiming to improve the costeffectiveness, environmental sustainability, and manufacturing process. Alternative methods based on green chemistry ariseto overcome these limitations and optimize the production of Fe_2O_3NPswith superior environmental performance, and more efficient processes[5,6,7]. The wide use of nanomaterials forenvironmental remediation includes the removal, stabilization, and degradation of different organic and inorganic contaminants such as heavy metals and organic matter[8]. Therefore, thepotential environmental impacts of nanomaterials, especially,iron-based nanoparticles, have to be considered and evaluated,which can affect different organisms and microorganisms in a large variety of ecosystems[9].Green chemistry, defined by Anastas and Warner in 1998 asthe design of environmentally friendly chemical processes andproducts[10] follows 12 principles summarized in the minimization of hazardous compounds and the generation of residues[11]. Along with sustainable chemistry, green chemistry improves the efficiency related to the use of natural resources, contributing from social, economic, and environmental[12].

Diabetic foot ulcer causing bacteria are one of the most important pathogens and considered a serious threat to public health in recent years. The toxic side effects of synthetic antibiotics have necessitated a search for new antibacterial agents.As far as our knowledge survey, no studies on the effect of nanoparticles against pathogenic bacteria that causing diabetic foot ulcer have been previously published. This prompted us to further investigate the antibacterial activity of iron oxide nanoparticles synthesized by pulsed laser ablation (Fe_2O_3NPs) against some pathogenic bacteria isolated from diabetic patients with recurrent diabetic foot in Baghdad Teaching Hospital, Iraq.

2.Materials and method

2.1 Sample collectionand bacterial diagnosis

Fifty samples from diabetic patients who suffer from recurrent diabetic foot in Baghdad Teaching Hospital were collected. For aerobic bacterial culture, samples were obtained aseptically by the use of sterilized swabs. To avoid isolation of colonizing bacterial flora, samples were obtained from the deepest part of the ulcer after the wound area was rinsed with saline and the wound was debrided. Samples were immediately transported to the microbiology laboratory for the required identification tests. All samples were cultured on different media. Isolated bacteria were identified by using different methods including cultural and microscopical characterization, in addition to biochemical tests. Then the diagnosis confirmed by using Vitek2 system.

2.2 Synthesis of Fe_2O_3NPs

eISSN 1303-5150

A high-purity Iron plate (about 99.95%) was immersed in 10 ml of deionized water in a Baekar beaker. A yttrium aluminum garnet (Nd: YAG) laser (New Wave Research, 1845L) is focused on a zinc plate surface with a wavelength of 532 nm, an energy of 100 mJ, and a laser stroke of 500, 1000 and 1500.) and the frequency rate is 6 Hz. As for the distance between the laser device and the surface of the zinc target, 12 cm. During the imaging process, the glass cup containing the Iron plate is periodically transferred to obtain colloidal homogeneous $\boldsymbol{fe_2o_3}$**NPs.**, respectively.

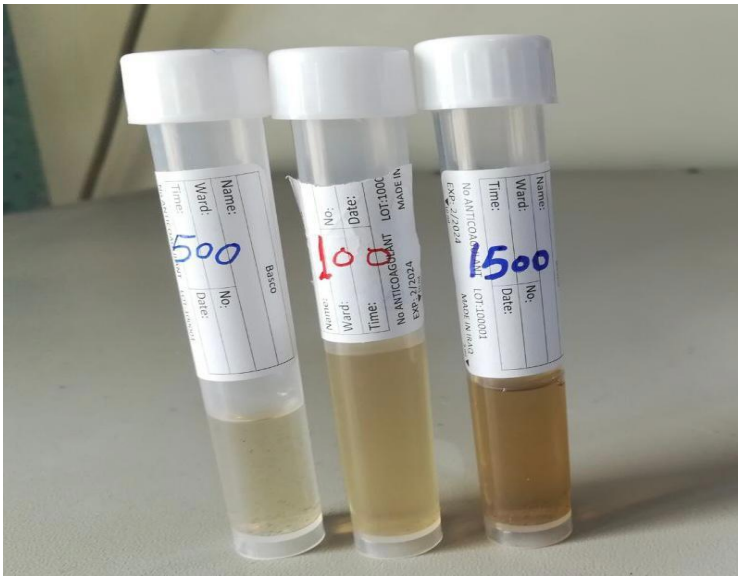

Figure (1) Preparation of Fe_2O_3 NPs at three an energy

2.3

optical properties

2.3.1**UV-vis**

The results showed that biosynthesized of Fe_2O_3NPs exhibited a maximum absorption peaks at 1500 pulses as shown in Figure 1.The result agree with (Fazio, Santoro et al. 2016)the iron oxidenanoparticles concentration were indirectly estimated carrying outoptical absorption measurements in the UV–vis spectral region (notshown) and also collecting, by means of a magnet, the particles onthe wall of the vial containing the colloidal solution. From Figure 2, we notice that the absorbance increases with the increase in the number of pulses, and this indicates an increase in the concentration of nanoparticles in the suspension, and this is consistent with the concentration results that were measured by the automatic absorption device, which was as in Table 1

eISSN 1303-5150

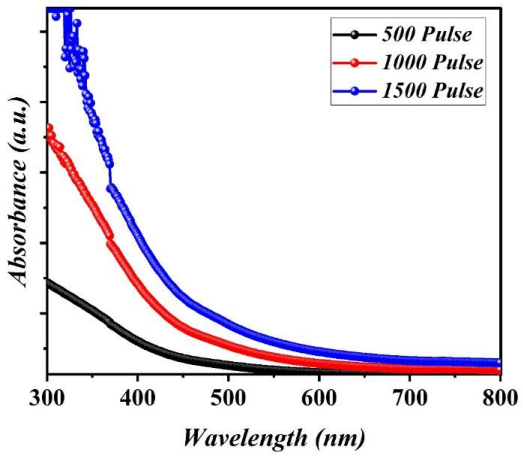

Figure2: UV-visible absorption spectra of IONPs **synthesized**

Table (1) represents the results of Atomic Absorption

N0	impulses	VALUE(Fe_2O_3) PPM
1	**500**	**19.9**
2	**1000**	**66.2**
3	**1500**	**47.75**

2.3.2

Energy Gap of Fe_2O_3NPs

In Figure (3), the energy gap of the Fe compound was calculated as a function of the number of pulses depending on the absorbance values, and it was from (2.1-2.6ev) and it was found that the energy gap lowering with the increase in the number of pulses and the reason is that by increasing the number of pulses, different particles sizes may have been removed compared to the number of pulses, and since the energy gap increases with decreasing in the particles sizes and this may be related to the lack of defects and the formation of sub energy levels within the energy gap.

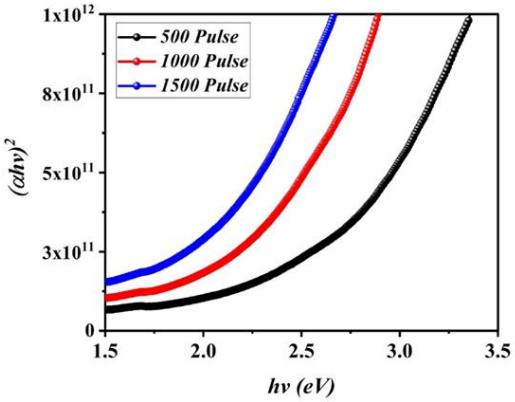

Figure 3: Energy Gap of fe_2o_3NPs

eISSN 1303-5150

2.3.3The X -ray diffraction of fe_2o_3 nanoparticles

The XRD spectra of Fe_2O_3NPs, nanoparticle powder is shown in Figure 4. The result where general spectra and the regions of these spectra are observed. Although Raman spectroscopy is a technique for studying atomic and molecular bonds physics of condensed matter, care must be taken when applying it to the study of iron oxides. Magnetite bands are not shown as in the direction patterns and in the XDR spectra, which may be due to the phase change from magnetite to hematite because excessive exposure of an iron oxide sample to laser radiation has been shown to generate hematite, indicating that some peaks with Fe_2O_3NPs phase could be attributed to this phenomenon(Santillán, Muñetón Arboleda et al. 2017).The peaks $\boldsymbol{fe_2o_3}$ NP in fig.4 were (33,36,49,58) and at 2θ = (211,110,202,018), respectively. Take note of the higher peak at (018). This is compatible with the card (33-0664), and the results show that the values of the element $\boldsymbol{fe_2o_3}$NP X-ray spectrum are consistent with the table (Joint Committee on Power Diffraction Standards) (JCPDS). The crystal size for $\boldsymbol{fe_2o_3}$NP was calculated using Scherre's Equation, and it was (17.44,61.86,78.38 nm), which corresponds to (500, 1000, 1500 pulses) respectively.

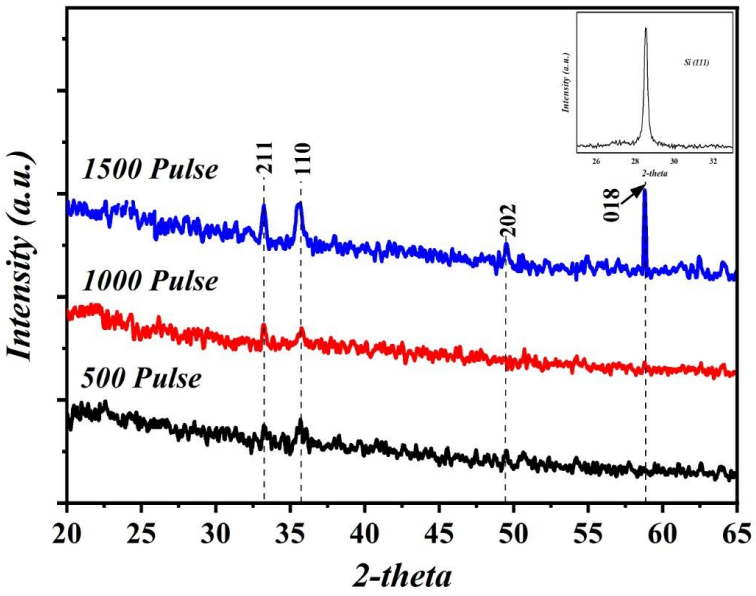

Figure 4 : : X-ray diffraction pattern of fe_2o_3NP

eISSN 1303-5150

2.3.4 Emission Scanning Electron Microscope

The Morphology and size reached (11 to 30) nm of Fe2O3 NPs were synthesis by pulsed laser method of the field emission scanning electron microscopy (Figure 5). The result according to[(Rivera-Chaverra, Restrepo-Parra et al. 2020)] IONP spherical shapes exhibited clustered with, size distribution ranging from 22 nm SEM nanoparticles was clustered with a mean diameter of 6 nm. shows that the morphology of the samples showed particles that are roughly spherical in shape, and have granulation and a tendency to agglomerate, confirming that the size of the particles was in the order of nanometers

963

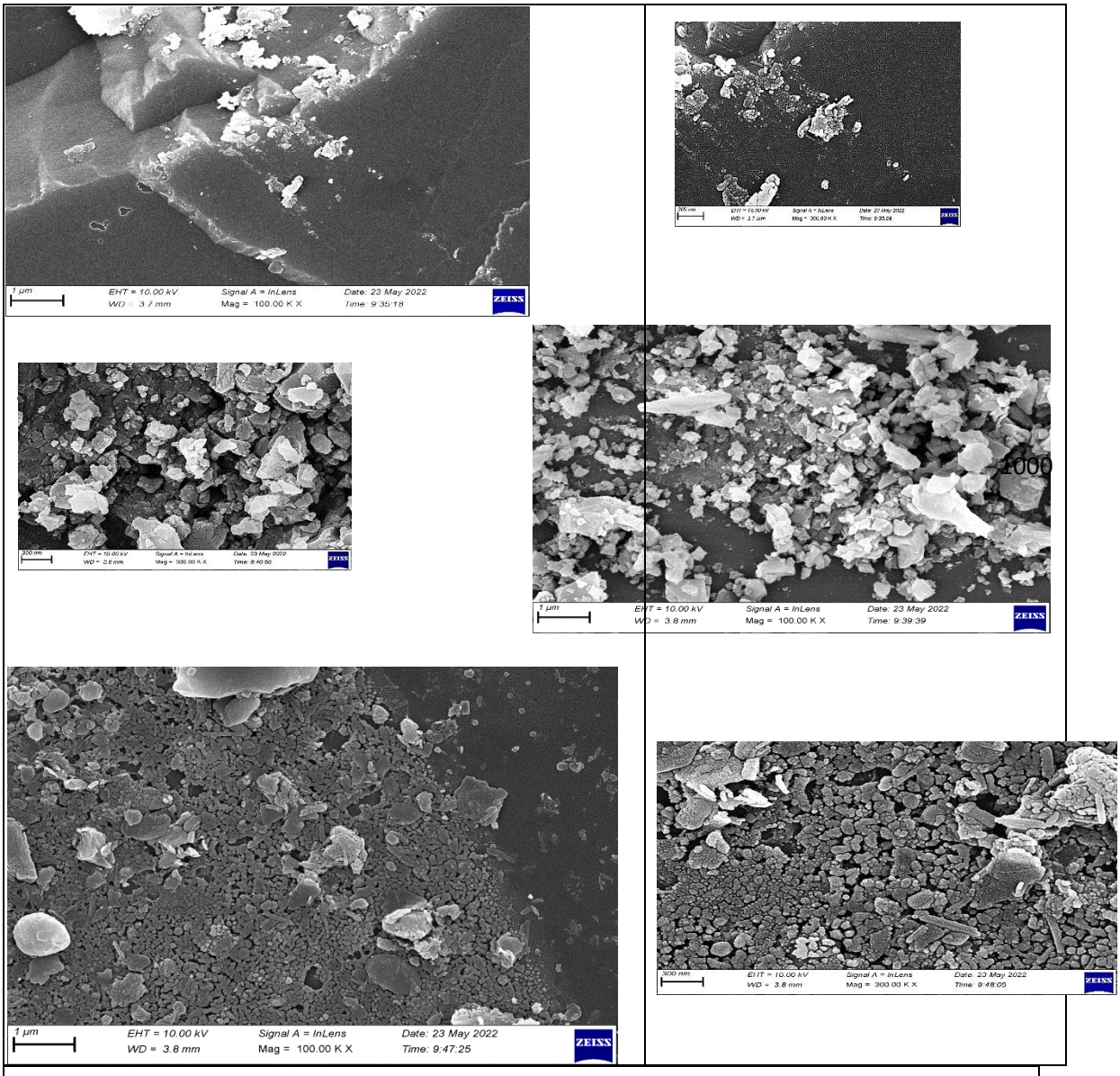

1500

Figure **5**: Field Emission Scanning Electron Microscope for fe_2o_3 NPs nanoparticles for laser strikes, (**A)** represents Fe 500, (**B)** represents Fe 1000, and (**C)** represents Fe1500

2.3.5 AFM

Atomic force microscope (AFM) images as shown in Figure 6 display the topography of the $\boldsymbol{fe_2o_3}$NPssurface, which agrees with the XRD result. The characterization results revealed that most of the Fe2O3 NPs are small size spherical particles. The mean diameter of the $\boldsymbol{fe_2o_3}$NPs synthesized in this study is 5.3 nm. Single surface plasmon resonance (SPR) peak revealed that the Fe2O3 NPs are mostly in the spherical shape,In this work, scanning probe microscope available AFM Measuring the granularity accumulation distribution, roughness, and grain size of the fe nanostructures range 40 to 90 nm showen in Figure 6. The size distribution of $\boldsymbol{fe_2o_3}$NPs is nearly Gaussian type shows agglomerates, the roughness was 11.55, 6.85, 20.36 for strikes 500, 1000, and 1500 respectively. It was found from the figures that the lowest granular size was at the pulse 500, and this is in agreement with the previous results that were clarified above.

(A)500

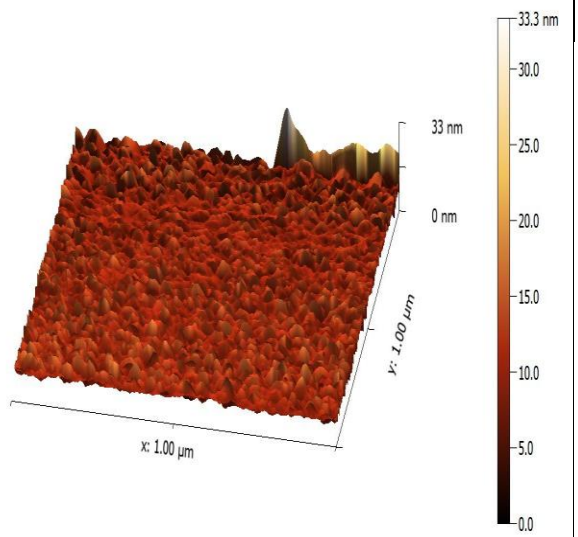

(B)1000

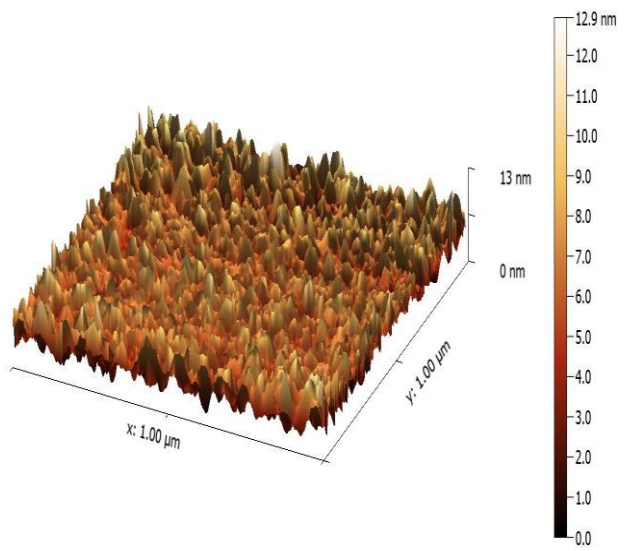

(C)1500

eISSN 1303-5150

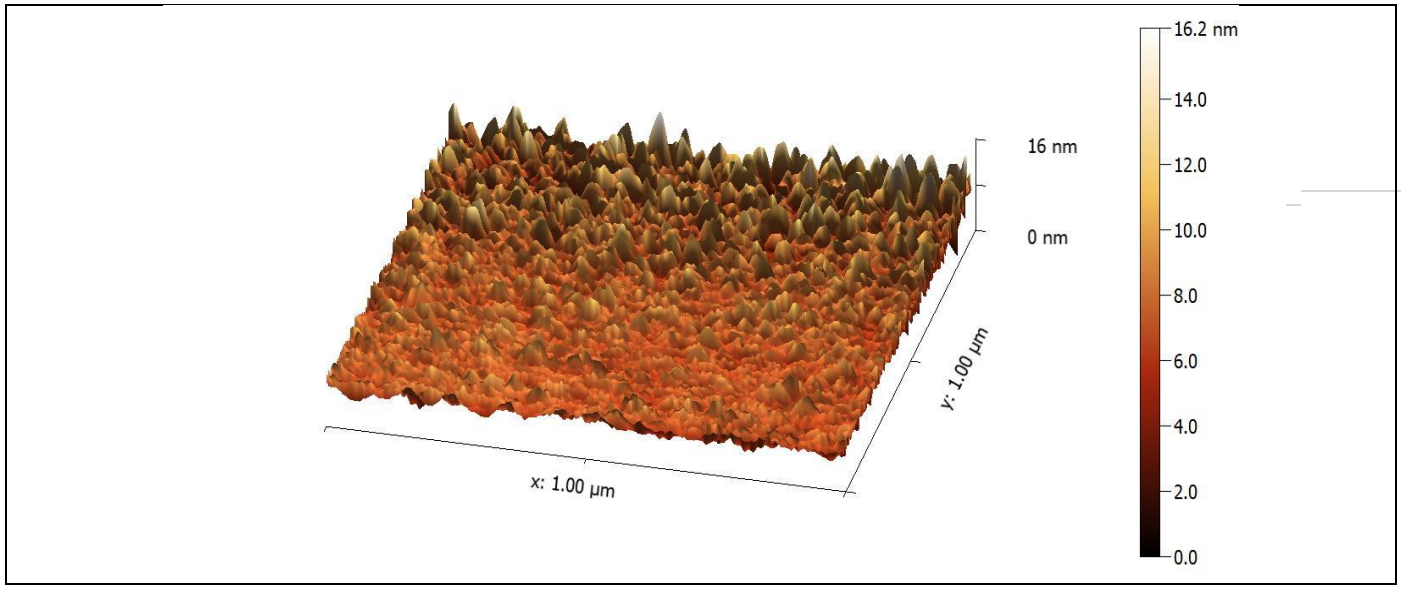

Figure(6): AFM for fe_2o_3 nanoparticles for laser strikes, (**A)** represents Fe 500 (**B)** represents Fe1000, and (**C)** represents Fe1500

2.3.6Antibacterial activity of the preparedfe_2o_3nanoparticles

Antibacterial activity of the prepared nanoparticles was done using agar well-diffusion assay.The agar plates cultured with tested bacteria(1.5×10^8) CFU/ml, wells cut into the plates with 6mm sterile cork borer were loaded with 20 µl of the way of fe_2o_3NPsat different concentration, the plates were incubated at 37°C for 24 hrs. Hindrance was identified by a zone of clearing around the supernatant well [Al-Gosha'ah, F. A., Al-Baker, S. M., & Al-Hetar, K. Y. (2014). Bacteriocin Typing of Staphylococcus aureus Isolated from Different Sources in Ibb City, Yemen. Jordan Journal of Biological Sciences,147(1570), 1-5]

3. Results and Discussion

Fifty swab samples were collected from diabetic patients who suffer from recurrent diabetic foot in Baghdad Teaching Hospital, the proportion of males was 65.3% and females 34.7%, and their age ranged between 38 and 70 years as showed in the table 2.

Table 2: number of patients with Isolates taken from them.

No.	Gender (No.)	Age (years)	No. of isolates
1	Male (1)	38	1
2	Femal (5)	43-47	12
	Male (7)		
3	Femal (6)	56-50	15
	Male (8)		
4	Femal (2)	63-59	13
	Male (11)		
5	Female (3)	70-65	11
	Male (7)		

eISSN 1303-5150

A total of 52 bacterial isolates were obtained. The isolated bacteria were *Pseudomonas luteola,Staphylococcus hominis, Aeromonas hydrophilia,Staphylococcus aureus, Escherichia coli, Klebsiella pneumoniae, Kocuriakristinae, Enterococcus faecalis, Sphingomonaspaucimobilis, Proteus penneri, Proteus vulgaris, and Proteus mirabilisr*(Table 3).

Table 3**: Isolated bacteria**

No.	Bacteria
1	***Pseudomonas luteola***
2	***Staphylococcus hominis***
3	***Aeromonas hydrophilia***
4	***Staphylococcus aureus***
5	***Escherichia coli***
6	***Klebsiella pneumoniae***
7	***Kocuriakristinae***
8	***Enterococcus faecalis***
9	***Sphingomonaspaucimobilis***
10	***Proteus penneri***
11	***Proteus vulgaris***
12	***Proteus mirabilis***

This result agrees with another previous study that has shown that males are more susceptible to foot infection than females [13, 14]. This might be due to factors such as variations in their lifestyles and work activities that force the feet to withstand greater pressure.While other result by [15] age of 40 years old all patients were over the. With sensory neuropathy, who are usually elderly. This might be because foot lesions in diabetic patients are more common in those.On the other hand,in Egypt also demonstrated a higher prevalence of Gve+ bacteria than Gve- bacteria in DFIs (65.5% vs. 34.5% and 67% vs. 30%, respectively [16].

The result by Hamid MH *et al*. [12] found that *K. pneumoniae* (47.8%) was the most prevalent Gve- in this study followed by P. mirabilis (30.4%) and Pseudomonas aeruginosa (13%), while E. coli and Proteus penneri (2.4% for each) were the least common.

The results showed that the prepared Fe_2O_3 NPshave antibacterial activity (Table 4). The highest inhibition zone diameters were(25.3±0.6,24.3±0.6,23.8±0.3,18.7±0.6, 18.5±0.5,17.5±0.9,16.0±0.9,15.8±0.8,15.7±0 .6,15.2±0.3,15.2±0.3,10.3±0.6) mm for nanoparticles (500 laser stroke) against*Proteus vulgaris*, *Proteus penneri, Sphingomonaspaucimobilis, Kocuriakristinae, Staphylococcus aureus, Proteus mirabilis, Klebsiella pneumoniae, Staphylococcus hominis, Escherichia coli,Pseudomonas aeruginosa, Enterococcus faecalis, Aeromonashydrophila,* respectively.

On the other hand, the diameters of inhibition zone were (21.7±1.2, 19.3±0.6, 16.2±0.3,15.5±0.5, 13.8±0.8, 12.7±0.6, 12.3±0.6,12.2±1.0, 9.3±0.6, 8.7±0.6)mmfornanoparticles (1000laserstroke) against *Proteus vulgaris*, *Proteus penneri, Pseudomonas aeruginosa, Kocuriakristinae,Sphingomonaspaucimobilis*

eISSN 1303-5150

, Staphylococcus hominis,Escherichia ***coli,*** *Enterococcus faecalis, Klebsiella pneumoniae,Staphylococcus aureus,*respectively.Moreover, the prepared$\boldsymbol{fe_2o_3}$NPsat a laser pulse 1500 had the lowest diameters of the inhibition zone when compared to others (Table 4).The antibacterial mode of action of NPs is generally described as adhering to one of the following mechanisms; cell plasma membrane damage, generation of reactive oxygen species, penetration of bacterial cytoplasmic membrane; and leading to intracellular effects such as interacting with deoxyribonucleic acid (DNA) and cell protein [18, 19, 20, 21,22].

Table 4: Antibacterial activity of the preparedFe_2O_3 NPsbased on virous laser pulses.

No.	Diameter of the inhibition zone (mm) (Mean±SD)		
	Fe 1500	**Fe 1000**	**Fe 500**
Aeromonashydrophila	0.0	0.0	10.3±0.6
Escherichia coli	10.3±0.6	12.3±0.6	15.7±0.6
Klebsiella pneumoniae	0.0	9.3±0.6	16.0±0. 9
Proteus mirabilis	0.0	0.0	17.5±0.9
Proteus penneri	17.3±0.6	19.3±0.6	24.3±0.6
Proteus vulgaris	19.3±0.6	21.7±1.2	25.3±0.6
Pseudomonas aeruginosa	12.7±0.6	16.2±0.3	15.2±0.3
Sphingomonaspaucimobilis	15.8±0.8	13.8±0.8	18.7±0.6
Enterococcus faecalis	10.7±0.6	[h]12.2±1.0	15.2±0.3
Kocuriakristinae	0.0	15.5+0.5	23.8±0.3
Staphylococcus aureus	0.0	8.7±0.6	18.5±0.5
Staphylococcus hominis	10.8±0.8	12.7±0.6	15.8±0.8

Figure 7: inhibition zones of *Aeromonashydrophila*after treatment with thefe_2o_3NPs.

Figure8:inhibition zones of *Staphylococcus aureus*after treatment with thefe_2o_3NPs.

eISSN 1303-5150

Reference

(1) Mai, T.; Hilt, J. Z. Functionalization of Iron Oxide Nanoparticles with Small Molecules and the Impact on Reactive Oxygen Species Generation for Potential Cancer Therapy. Colloids Surf., A 2019, 576, 9−14.

(2) Sun, X.; Alcaraz, N.; Qiao, R.; Hawley, A.; Tan, A.; Boyd, B. J. Magnetically-Stimulated Transformations in Nanostructure of Lipid Mesophases: Effect of Structure of Iron Oxide Nanoparticles. Colloids Surf., B 2020, 191, 110965.

(3) Nguyen, M. P.; Nguyen, M. H.; Kim, J.; Kim, D. Encapsulation of Superparamagnetic Iron Oxide Nanoparticles with PolyaspartamideBiopolymer for Hyperthermia Therapy. Eur. Polym. J. 2020, 122, 109396.

(4) Moldes-Diz, Y.; Eibes, G.; Vázquez-Vázquez, C.; Fondado, A.; Mira, J.; Feijoo, G.; Lema, J. M.; Moreira, M. T. A Novel Enzyme Catalysis Reactor Based on Superparamagnetic Nanoparticles for Biotechnological Applications. J. Environ. Chem. Eng. 2018, 6, 5950−5960.

(5) Feijoo, S.; González-García, S.; Moldes-Diz, Y.; Vazquez- Vazquez, C.; Feijoo, G.; Moreira, M. T. Comparative Life Cycle Assessment of Different Synthesis Routes of Magnetic Nanoparticles. J. Clean. Prod. 2017, 143, 528−538.

(6) Su, B.; Lin, J.; Owens, G.; Chen, Z. Impact of Green Synthesized Iron Oxide Nanoparticles on the Distribution and Transformation of As Species in Contaminated Soil. Environ. Pollut. 2020, 258, 113668.

(7) Rajiv, P.; Bavadharani, B.; Kumar, M. N.; Vanathi, P. Synthesis and Characterization of Biogenic Iron Oxide Nanoparticles Using Green Chemistry Approach and Evaluating Their Biological Activities. Biocatal. Agric. Biotechnol. 2017, 12, 45−49.

(8) Caramazana, P.; Dunne, P.; Gimeno-Fabra, M.; McKechnie, J.;Lester, E. A Review of the Environmental Impact of Nanomaterial Synthesis Using Continuous Flow Hydrothermal Synthesis. Curr. Opin. Green Sustain. 2018, 12, 57−62.

(9) Gong, X.; Huang, D.; Liu, Y.; Peng, Z.; Zeng, G.; Xu, P.; Cheng, M.; Wang, R.; Wan, J. Remediation of Contaminated Soils by Biotechnology with Nanomaterials: Bio-Behavior, Applications, and Perspectives. Crit. Rev. Biotechnol. 2018, 38, 455−468.

(10) Rónavári, A.; Balázs, M.; Tolmacsov, P.; Molnár, C.; Kiss, I.; Kukovecz, Á.; Kónya, Z. Impact of the Morphology and Reactivity of Nanoscale Zero-Valent Iron (NZVI) on Dechlorinating Bacteria.Water Res. 2016, 95, 165−173.

(11) de Marco, B. A.; Rechelo, B. S.; Tótoli, E. G.; Kogawa, A. C.; Salgado, H. R. N. Evolution of Green Chemistry and Its Multidimensional Impacts: A Review. Saudi Pharm. J. 2019, 27, 1−8.

(12) Whiteker, G. T. Applications of the 12 Principles of Green Chemistry in the Crop Protection Industry. Org. Process Res. Dev. 2019, 23, 2109−2121.

eISSN 1303-5150

13. Anvarinejad, M., et al., *Isolation and antibiotic susceptibility of the microorganisms isolated from diabetic foot infections in Nemazee Hospital, Southern Iran.* Journal of pathogens, 2015. 2015.

14. Lipsky, B.A., R.E. Pecoraro, and J.H. Ahroni, *Foot ulceration and infections in elderly diabetics.* Clinics in geriatric medicine, 1990. 6(4): p. 747-769.

15. Perriere, J., et al., *Comparison between ZnO films grown by femtosecond and nanosecond laser ablation.* Journal of Applied Physics, 2002. 91(2): p. 690-696.

16. Noha, A.K., et al., *Antibacterial resistance pattern of aerobic bacteria isolated from patients with diabetic foot ulcers in Egypt.* African Journal of Microbiology Research, 2014. 8(31): p. 2947-2954.

17. Dutta, R.K., et al., *Studies on antibacterial activity of ZnO nanoparticles by ROS induced lipid peroxidation.* Colloids and Surfaces B: Biointerfaces, 2012. 94: p. 143-150.

18.Loo YY, Rukayadi Y, Nor-Khaizura MA, Kuan CH, Chieng BW, Nishibuchi M, Radu S. (2018). *In Vitro* Antimicrobial Activity of Green Synthesized Silver Nanoparticles Against Selected Gram-negative Foodborne Pathogens. Frontiers in Microbiolgy, 16(9):1555. doi: 10.3389/fmicb.2018.01555. PMID: 30061871; PMCID: PMC6054941.

19. Gabrielyan L., Badalyan H., Gevorgyan V., Trchounian A. (2020). Comparable antibacterial effects and action mechanisms of silver and iron oxide nanoparticles on *Escherichia coli* and *Salmonellatyphimurium*. Scientific Reports, 10: 13145. doi.org/10.1038/s41598-020-70211-x

20. Slavin YN, Asnis J, Häfeli UO, Bach H. (2017). Metal nanoparticles: understanding the mechanisms behind antibacterial activity. Journal of Nanobiotechnology, 3;15(1):65. doi: 10.1186/s12951-017-0308-z. PMID: 28974225; PMCID: PMC5627441.

21. Wang L., Hu C., Shao L. (2017). The antimicrobial activity of nanoparticles: present situation and prospects for the future, a review. International Journal of Nanomedicine, 12: 1227–1249.

22. Joshi A.S., Singh P., Mijakovic I. (2020). Interactions of Gold and Silver Nanoparticles with Bacterial Biofilms: Molecular Interactions behind Inhibition and Resistance, a review. International Journal of Molecular Sciences, 21, 7658, doi:10.3390/ijms21207658

Fazio, E., et al. (2016). "Iron oxide nanoparticles prepared by laser ablation: Synthesis, structural properties and antimicrobial activity." Colloids and Surfaces A: Physicochemical and .Engineering Aspects**490**: 98-103

Santillán, J. M., et al. (2017). "Optical and magnetic properties of Fe nanoparticles fabricated by femtosecond laserablation in organic and inorganic solvents." ChemPhysChem**18**(9): 1192-1209

Rivera-Chaverra, M. J., et al. (2 .(020 "Synthesis of oxide iron nanoparticles using laser ablation for possible hyperthermia applications." Nanomaterials**10**(11): 2099.